ATLANTIS PRESS
Advances in Intelligent Systems Research, volume 165
International Conference on Modeling, Simulation, Optimization and Numerical Techniques (SMONT 2019)

Simulation of Thermally Assisted Cutting of the Aluminum Alloy after WAAM

Hongyu Tian[1,2,*], Zhenyang Lu[1,2], Shujun Chen[2] and Xu Yu[2]
[1]College of Robotics, Beijing Union University, Beijing, 100020, China
[2]College of Mechanical Engineering and Applied Electronics Technology, Beijing University of Technology, Beijing, 100124, China
*Corresponding author

***Abstract*—A hybrid technique of additive manufacturing and subtractive process has provided a new solution combining product design and control by software. Wire Arc Additive Manufacturing (WAAM) process wins well-respected because of its low cost and high efficiency of deposition, nevertheless the process has its limitation of high heat input and low forming accuracy. A new process of additive manufacturing with high efficiency of modeling is urgent needed which can control heat transfer, mass transfer and force transfer. To overcome the disadvantage upon, various hybrid manufacturing techniques have been developed with high efficiency and controlled modeling in recently. The machining process in hybrid manufacturing has more different characteristics from traditional material removal processes, such as residual stress and heat in the blank. These influence the whole efficiency of the hybrid manufacturing. The primary purpose of this study is to explore the feasibility of thermal machining during this process and make rational use of AM in order to obtain optimal accuracy.**

Keywords—surface roughness predictive; thermally assisted cutting; modelling and simulation; RSM; WAAM

I. INTRODUCTION

Traditional manufacturing processes often lead to high processing rates, which can not meet the growing demands of sustainable, low-cost and environmentally friendly modern industries. Additive Manufacturing Technology (AM), as a promising technology, has attracted wide attention. Because of the low cost of equipment and high deposition rate, innovative welding wire and arc additives have significant advantages over other materials that can be used to deposit many connectable materials, such as carbon steel, aluminium alloy, nickel alloy and titanium alloy.

According to the heat source classification of molten wire, the manufacturing process of arc additives can be divided into gas shielded tungsten arc welding (GTAW), plasma arc welding (PAW) and gas shielded metal arc welding (GMAW) [1]. These methods can produce three-dimensional metal parts with high density and good bonding strength. [2]. However, due to the effect of ladder effect and the fluidity of molten metal, it is still difficult to manufacture parts with the same geometric accuracy and surface quality as traditional processing technology regardless of the energy and feedback [3]. A hybrid of additive manufacturing and subtractive process has provided a fundamental solution to overcome the disadvantages most [4]. In recent years, various hybrid manufacturing technologies have been developed, such as hybrid layered manufacturing [5], hybrid plasma deposition and milling [6], three-dimensional welding and milling [7].

In order to obtain good morphology and high efficiency, the subtractive process can be carried out when the work-piece is still under additive manufacturing processing waste heat. Some researches are given that higher temperature can make the cutting smoothly [8]. Because of the soften work-piece and the reduced yield strength, the basic research of thermally subtractive cutting is discussed in this paper. Predicting the modelling of surface roughness and simulating the orthogonal cutting of the thermally milling process are provided. Based on Response Surface Methodology (RSM), scientific experiments were designed to improve the feasibility of the thermally machining of 2219 aluminum alloy after WAAM. Optimization parameters for cutting process consisted of work-piece temperature, feed per tooth and spindle speed.

II. EXPERIMENTAL

A. Materials and System

The chemical composition of 2219 aluminium alloy used in this study is shown in Table 1. A 2219 aluminium alloy plate with thickness of 10 mm was fabricated in this experiment. The size of the plate is 380 mm × 320 mm × 10 mm.

TABLE I. CHEMICAL COMPOSITIONS OF 2219 ALUMINUM ALLOY (WT. %)

Cu	**Si**	**Fe**	**Mn**	**Mg**	**V**	**Zr**	**Zn**	**Ti**	**Others**	**Al**
5.8—6.8	≤ 0.2	≤ 0.3	0.2—0.4	≤ 0.02	0.05—0.15	0.1—0.25	≤ 0.1	0.02—0.1	≤ 0.15	Bal.

The milling robot is KR500 (Ogsburg Kuka Co., Ltd., Bavaria, Germany), which is suitable for milling applications equipped with high-speed motorized spindle ES779 (to provide maximum spindle speed: 22000 rpm). The standard cutting tool was applied by 3-flute solid carbide flat-end mill with a helix angle of 60° and a diameter of 10 mm axis. To simulate thermally assisted machining of the work-piece, a heating system was mounted to the robot positioner which is displayed in Figure I.

Copyright © 2019, the Authors. Published by Atlantis Press.
This is an open access article under the CC BY-NC license (http://creativecommons.org/licenses/by-nc/4.0/).

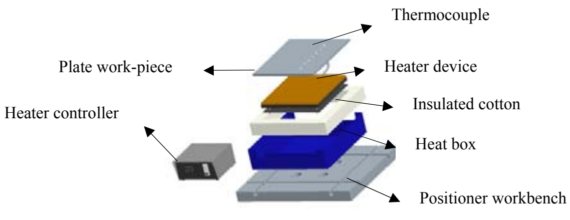

FIGURE I. EXPLODED-VIEW OF HEATING SYSTEM FOR THERMAL MACHINING

The surface roughness of work-piece under different processing conditions was measured by TR200 surface roughness tester.

B. *Experimental Design for Thermally Assisted Cutting*

The processing parameters considered in end milling process include spindle speed, feed speed and work temperature. These three dependent variables are investigated using RSM. The response is the surface roughness parameter *R*a. The Central Composite Design (CCD) for RSM required only five levels, coded as -α, -1, 0, +1, +α. In order to improve prediction accuracy, rotatable design is used while a value of α is 1.682. The total number of experiments designed are 20 based on the five levels and a three-factor experimental design. The selected process variables and bounds are presented in Table II.

TABLE II. PROCESS VARIABLES AND BOUNDS

	Name	Units	Low	High	-alpha	+alpha
Factor A	*fz*	mm/s	0.0181	0.0419	0.01	0.05
Factor B	*n*	r/min	1006.75	2493.25	500	3000
Factor C	*Temp.*	℃	110.809	289.191	50	350
Response 1	*Ra*	μm	0.5693	2.5398		
Response 2	*Rz*	μm	3.2068	27.401		

III. RESULTS AND DISCUSSION

The experimental results of surface roughness were analyzed by ANOVA to determine the parameters that significantly affect the surface roughness, and were analyzed by software package design experts (Design Experts 8.0.7, 2010, Stat-Ease Inc., Minnepolis). The significance level of the analysis was 0.05 (95% confidence level). Analysis of variance values are presented in Table Ⅲ. The model F-value of 5.23 implies the model is significant. A large level of "Model F-value" could occur due to noise and in this experiment it is only a 0.82% chance. The Lack of Fit value of 0.17 indicates its not significant relation to the pure error. A large "Lack of Fit F-value" level could result in noise, while a 96.21% chance in this study. There is a Non-significant lack of fit is the ideal result.

TABLE III. ANALYSIS OF VARIANCE TABLE FOR RA

Source	Sum of squares	df	Mean square	F-value	p-value
Model	4.29	9	0.48	5.23	0.0082 Significant
A-feed	1.04	1	1.04	11.46	0.0069
B-speed	1.45	1	1.45	15.92	0.0026
C-temp.	0.075	1	0.075	0.82	*0.3855*
AB	0.083	1	0.083	0.91	*0.3634*
AC	0.30	1	0.30	3.34	*0.0977*
BC	1.278e-3	1	1.278e-3	0.014	*0.9081*
A^2	0.36	1	0.36	3.95	*0.0749*
B^2	2.164e-3	1	2.164e-3	0.024	*0.8806*
C^2	1.07	1	1.07	11.72	0.0065
Residual	0.91	10	0.091		
Lack of fit	0.13	5	0.027	0.17	*0.9621* Not significant
Pure error	0.78	5	0.16		
Cor total	5.20	19			

From analysis of variance in Table Ⅲ, some parameters are not significant. The modelling of surface roughness *R*a can be simplified to Eq. (1).

$$Ra = 1.51 + 32.54 f_z - (7.41 \times 10^{-4}) \cdot n \\ - (3.42 \times 10^{-5}) \cdot T^2 \qquad (1)$$

As a function of 2 factors at a time, the three-dimensional surface graphs are given. Figure Ⅱ shows the surface plot of surface roughness Ra with variation in the values of speed (B) and temperature (C). It is observed that as the spindle speed increases from 1898.7 to 2493.3rpm the roughness value reduces from 1.4 to 1.8μm. The surface roughness increases firstly and then decreases. As the spindle speed increases from 1006.8 to 1898.7rpm the roughness value increases from 1.8 to 2.2μm. As the spindle speed is low the roughness changes slowly with the temperature based the contour plot. And the roughness varies rapidly with the temperature when the spindle speed is high. The optimal surface roughness can be obtained based on high spindle speed.

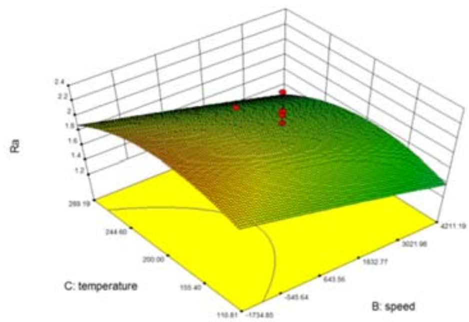

FIGURE II. 3D SURFACE PLOT OF RA FOR B AND C

IV. FE-SIMULATION

A. *Finite Element Simulation Model*

To research the sensibility of temperature, the thermally assisted milling process was simulated by ABAQUS/Standard with two dimensional orthogonal cutting under plane strain conditions. The commercial finite element software can be used to study the effect of accumulated strain and temperature caused by processing steps on the final contour of residual stress. Material constitutive model is a Johnson-Cook model [9] which reflects the constitutive behavior of metals under high strain, high strain rate and high temperature. Eq. (2) shows the model.

$$\sigma = f(\varepsilon)\cdot f(\dot{\varepsilon})\cdot f(T) = (A+B\varepsilon^n)[1+C\ln(\frac{\dot{\varepsilon}}{\dot{\varepsilon}_0})][1-(\frac{T-T_r}{T_m-T_r})^m] \quad (2)$$

The parameter ε is equivalent plastic strain, parameter $\dot{\varepsilon}_0$ is reference strain rate, and parameter $\dot{\varepsilon}$ is equivalent plastic strain rate. The parameter σ is equivalent plastic stress. The parameter T_m is the melting temperature of material, and parameter T is dynamic temperature. And parameter T_r is the room temperature [10]. The constant A is initial yield stress, B is hardening modulus, C is strain rate dependence coefficient, n is work hardening index, and m is thermal softening coefficient [11]. Aluminum alloy materials parameters constant A, B, C, n , and m which could obtain from tensile tests. They are showed in Table IV. The finite element computational analysis parameters applied list in Table V, in which Al alloy matrix is modeled as a thermal-elastic-plastic material.

TABLE IV. MATERIAL CONSTANTS FOR THE JOHNSON-COOK CONSTITUTIVE EQUATION OF 2219 AL

Matrix material	A (MPa)	B (MPa)	C	n	m	T_m (K)	T_r (K)
2219 Al	170	228	0.028	0.31	2.75	816	298

TABLE V. MATERIAL PARAMETERS FOR THE ANALYSIS

Material properties	2219 Al	Cutting tool (YG8)
Density (kg · m^{-3})	2840	14500
Modulus of elasticity (GPa)	70	650
Poisson's ratio	0.30	0.25
Coefficient of thermal expansion (×10^{-6}K^{-1})	23.0	4.9
Thermal conductivity (W · m^{-1} · K^{-1})	116	59
Specific heat capacity (J · kg^{-1} · K^{-1})	900	334

Parameter D is defined as a damage of one element in the model of the Johnson-Cook. When the condition in Eq. (3) was satisfied, the chip of model would be separated.

$$D=\sum\frac{\Delta\varepsilon}{\varepsilon^f}=1 \quad (3)$$

The change of the equivalent plastic strain named $\Delta\varepsilon$ in Eq. (3) and the equivalent strain to the fracture named ε^f . A function of the temperature, equivalent stress, strain change rate, and pressure are expressed in Eq. (4) [12].

$$\varepsilon^f=[d_1+d_2\exp(d_3\sigma^*)][1+d_4\ln(\frac{\dot{\varepsilon}}{\dot{\varepsilon}_0})][1+d_5(\frac{T-T_r}{T_m-T_r})] \quad (4)$$

The parameters d_1...d_5 are the failure parameters, which can be obtained from the damage tests of relevant researches and are listed in Table VI. FE model of the tool-work-piece couple for the numerical assessment is showed in Figure III.

TABLE VI. FAILURE PARAMETERS OF 2219 AL

Matrix material	d_1	d_2	d_3	d_4	d_5
2219 Al	0.13	0.10	-1.5	0.01	0.1

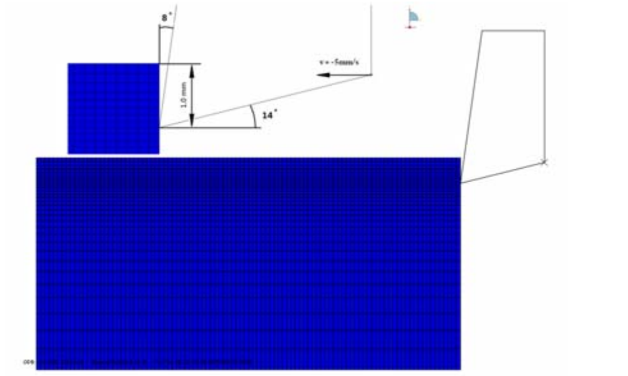

FIGURE III. FE MODEL OF THE TOOL-WORK-PIECE COUPLE

B. Finite Element Simulation Results

Figure IV shows some simulation results of Von Mises stress and chip formation at 1.0mm chip thickness for thermal milling with cutting velocity of 5mm/s and edge radius of 0.01mm. It is observed that the maximum stress of chip was located near the tool-chip interface named the primary shear zone. Figure V shows the change curve of maximum Von Mises stress in different initial temperatures of work-piece. It can be seen that the stress decreases by increasing the initial temperature.

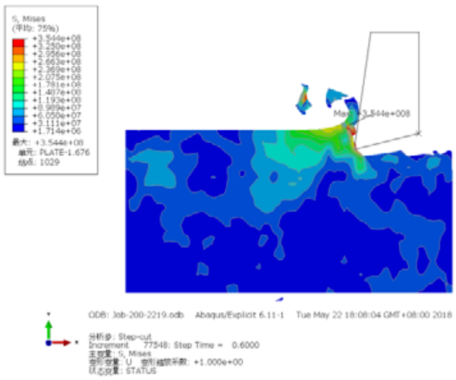

a) Initial temperature of work-piece is 200℃

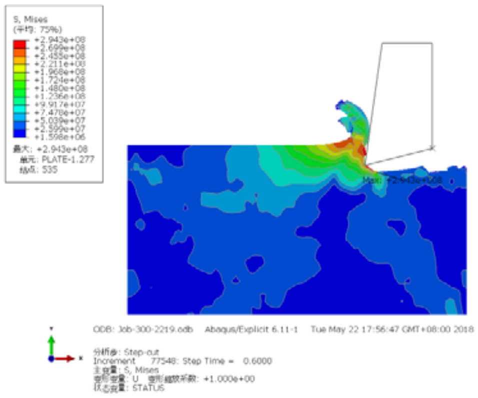

b) Initial temperature of work-piece is 300℃

FIGURE IV. SIMULATION OF MISES STRESS FOR THERMAL CUTTING

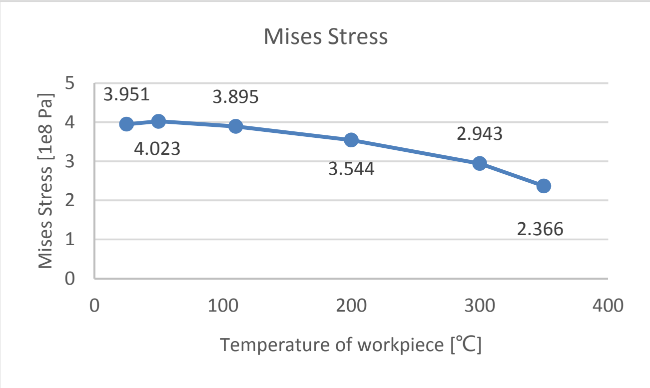

FIGURE V. MISES STRESS IN DIFFERENT TEMPERATURE OF WORK-PIECE

V. CONCLUSIONS

This work proposed a multi-objective solution for the minimization of surface roughness in a hybrid manufacturing process combining WAAM and milling. Cutting process parameters of this thermally assisted milling in hybrid process were optimized including feed per tooth, spindle speed and temperature of work-piece. Experiments were planned using the response surface methodology in five levels for the milling of AA2219. A sensibility analysis to temperature is carried out by means of finite element method to simulation the Von Mises stresses of thermal cutting by ABAQUS/Standard. Based on above studies the following conclusions were made:

1) The mathematical model developed in the work gives good co-relation between the process parameters and the responses. The predicted model of surface roughness indicates that the temperature is a significant parameter in thermal cutting.

2)The results of ANOVA and confirmation experiments have proved that the mathematical models of surface roughness in different temperature are well-fitted and the estimated values of the responses are closer to the investigation's results with 95% confidence level.

3)Experiments show that higher spindle speed and lower feed rate can achieve a satisfactory surface roughness. It is observed that the surface roughness increases firstly and then decreases with the temperature of the work-piece which can reach the finished or semi-finish machining level.

4)It can be seen that the stress of cutting tool decreases by increasing the initial temperature from the results of simulation.

5)The results of the mathematical prediction and finite element simulation prove the feasibility of thermal cutting after WAAM.

ACKNOWLEDGMENT

This paper was supported by the National Natural Science Foundation of China (No. 51475008, 51775007), the China Postdoctoral Science Foundation funded project (No. 2017M610726) and the Major national special projects of China (No. 2014zx04001-171) .

REFERENCES

[1] Xiong J, Li R, Lei Y, et al. Heat propagation of circular thin-walled parts fabricated in additive manufacturing using gas metal arc welding[J]. Journal of Materials Processing Technology, 2017, 251.

[2] Mughal, M.P., Fawad, H., Mufti, R.A., Three-dimensional finite-element modelling of deformation in weld-based rapid prototyping. Proc. Inst. Mech. Eng.: Mech. Eng Sci.220(6), 2006, 875-885.

[3] Kumbhar N N, Mulay A V. Post Processing Methods used to Improve Surface Finish of Products which are Manufactured by Additive Manufacturing Technologies: A Review[J]. Journal of the Institution of Engineers, 2016:1-7.

[4] Flynn, J.M.; Shokrani, A.; Newman, S.T.; Dhokia, V. Hybrid additive and subtractive machine tools—Research and industrial developments. Int. J. Mach. Tools Manuf. 2016, 101, 79–101.

[5] Kapil, S.; Legesse, F.; Kulkarni, P.; Joshi, P.; Desai, A.; Karunakaran, K.P. Hybrid-layered manufacturing using tungsten inert gas cladding. Prog. Addit. Manuf. 2016, 1, 79–91.

[6] Xiong, X.; Zhang, H.;Wang, G.;Wang, G. Hybrid plasma deposition and milling for an aeroengine double helix integral impeller made of superalloy. Robot. Comput. Integr. Manuf. 2010, 26, 291–295.

[7] Song, Y.; Park, S.; Choi, D.; Jee, H. 3D welding and milling: Part I—A direct approach for freeform fabrication of metallic prototypes. Int. J. Mach. Tools Manuf. 2005, 45, 1057–1062.

[8] Sun S, Brandt M, Dargusch M S. Thermally enhanced machining of hard-to-machine materials—A review[J]. International Journal of Machine Tools & Manufacture, 2010, 50(8):663-680.

[9] Johnson GR, Cook WH. A construetive model and data for metals subjected tolarge strains, high strain rates and high temperatures. Proc Seventh Int Sympos Ballist 1983:541–7.

[10] Chunzheng Duan, Wei Sun, Cheng Fu, et al. Modeling and simulation of tool-chip interface friction in cutting Al/SiCp composites based on a three-phase friction model[J]. International Journal of Mechanical Sciences, 2018, 142-143:384-396.

[11] Fan Y H, Wang T, Hao Z P, et al. Surface residual stress in high speed cutting of superalloy Inconel718 based on multiscale simulation[J]. Journal of Manufacturing Processes, 2018, 31:480-493.

[12] Zhou L, Cui C, Zhang PF , Ma ZY . Finite element and experimental analysis of machin- ability during machining of high-volume fraction SiCp/Al composites. Int J Adv Manuf Tech 2017;91:1935–44 .